Article

pubs.acs.org/Biomac

Antibacterial Surfaces Based on Polymer Brushes: Investigation on the Influence of Brush Properties on Antimicrobial Peptide Immobilization and Antimicrobial Activity

Guangzheng Gao,[†] Kai Yu,[†] Jason Kindrachuk,[‡] Donald E. Brooks,[†,§] Robert E. W. Hancock,[‡] and Jayachandran N. Kizhakkedathu*[,†,§]

[†]Centre for Blood Research and Department of Pathology and Laboratory Medicine, 2350 Health Sciences Mall, University of British Columbia, Vancouver, British Columbia, Canada V6T 1Z3

[‡]Centre for Microbial Diseases and Immunity Research, Department of Microbiology and Immunology, University of British Columbia, 2259 Lower Mall Research Station, Vancouver, British Columbia, Canada V6T 1Z3

[§]Department of Chemistry, University of British Columbia, Vancouver, British Columbia, Canada V6T 1Z3

Supporting Information

ABSTRACT: Primary amine containing copolymer, poly(*N*,*N*-dimethylacrylamide-*co*-*N*-(3-aminopropyl)-methacrylamide hydrochloride) (poly(DMA-*co*-APMA)), brushes were synthesized on Ti surface by surface-initiated atom transfer radical polymerization (SI-ATRP) in aqueous conditions. A series of poly(DMA-*co*-APMA) copolymer brushes on titanium (Ti) surface with different molecular weights, thicknesses, compositions, and graft densities were synthesized by changing the SI-ATRP reaction conditions. Cysteine-functionalized cationic antimicrobial peptide Tet213 (KRWWKWWRRC) was conjugated to the copolymers brushes using a maleimide−thiol addition reaction after initial modification of the grafted chains using 3-maleimidopropionic acid *N*-hydroxysuccinimide ester. The modified surfaces were characterized by X-ray photoelectron spectroscopy (XPS), water contact angle measurements, attenuated total reflectance Fourier transform infrared (ATR-FTIR) spectroscopy, atomic force microscopy (AFM), and ellipsometry analysis. The conjugation of the Tet213 onto brushes strongly depended on graft density of the brushes at different copolymer brush compositions. The peptide density (peptides/nm^2) on the surface varied with the initial composition of the copolymer brushes. Higher graft density of the brushes generated high peptide density (pepetide/nm^2) and lower number of peptides/polymer chain and vice versa. The peptide density and graft density of the chains on surface greatly influenced the antimicrobial activity of peptide grafted polymer brushes against *Pseudomonas aeruginosa*.

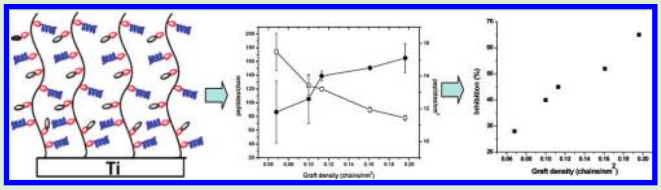

1. INTRODUCTION

Infections associated with post implantation and catheterization poses a significant threat to patients and a serious challenge to clinicians. High infection rates are observed for orthopedic implants, stents, urinary catheters, venous catheters, etc.[1−7] The origins of these infections are mostly due to bacterial adhesion and proliferation on synthetic surfaces which these devices are made up of.[2,4,8] The situation and treatments can be further problematic if encapsulation of the devices occur which prevent the diffusion of antibiotics to the infection site and leads to decrease in the efficiency of these agents.[7,8] The existence of drug resistant bacteria such as methicillin-resistant *Staphylococus aureus* (MRSA) complicates the condition further. Thus, the development of methods which localizes the action antimicrobial agents on the surface of biomaterials is very attractive.

Functional surface coatings based on polymer brushes have gained tremendous attention in recent years due to their excellent long-term stability owing to high mechanical and chemical robustness.[9,10] Importantly, such polymer brush coatings can be applied to most of the currently used biomedical materials including plastics, metals, and ceramics as demonstrated in the development of protein resistant and antithrombotic surfaces.[9−17] Hydrophilic polymer brush coatings have shown excellent biocompatibility[14−17] and cell-adhesion resistance,[18] and it can be modified with either proteins or peptides to generate biomimicking surfaces.[18,19] Hence, polymer brush coatings are very attractive choice for the development of next generation implant coatings.

Antimicrobial peptides (AMPs) are an attractive choice for the replacement of current antibiotics due to their board spectrum activity and relatively nontoxic nature toward host cells.[20−22] It has been suggested that bacteria will only develop resistance to these peptides slowly due to their complex mechanisms of action. Recently, we developed through large-scale screening new generation (AMPs) with broad spectrum activity against Gram-negative and Gram-positive bacteria, which were active on surfaces.[23,24] Very recently, we have

Received: July 13, 2011
Revised: September 7, 2011
Published: September 8, 2011

shown that AMPs are active on surfaces both in vitro and in vivo.[25]

Although polymer brushes were used as a method for the covalent attachment of the AMPs recently by our group and others,[25−27] no structure−property correlations with respect to polymer brushes have been reported to date. In this study, we investigated the influence of polymer brush properties on the conjugation of an antimicrobial peptide Tet213 and the antimicrobial properties of the peptide conjugated surface. Primary amine-functionalized copolymer brushes were synthesized by surface-initiated atom transfer radical polymerization (SI-ATRP). The functional brushes were subsequently modified to attach cysteine-terminated peptide using a Michael-type addition reaction. The properties of the grafted polymer and peptide conjugated surfaces were characterized by water contact angle measurements, XPS, ellipsometry, ATR-FTIR, and atomic force microscopy analyses. The antimicrobial activity of Tet213 conjugated polymer layer was correlated with the structure of the copolymer brush.

2. EXPERIMENTAL SECTION

2.1. Materials. 3-Aminopropyltriethyoxysilane (APTES) (98%), 1,1,4,7,10,10-hexamethyltriethylenetetramine (HMTETA) (97%), 2-chloropropionyl chloride (97%), methyl 2-chloropropionate (97%), CuCl (99%), and $CuCl_2$ (99%) were purchased from Aldrich (Oakville, ON). *N*-(3-Aminopropyl)methacrylamide hydrochloride (APMA) (98%) and 3-maleimidopropionic acid *N*-hydroxysuccinimide ester (SMP) (97%) were purchased from Polysciences and used as supplied. *N,N*-Dimethylacrylamide (DMA) (Aldrich, 99%) was distilled at reduced pressure before use. Water was purified by Mili-Q Plus water purification system (Milipore Corp., Bedford, MA). All other reagents were purchased from Aldrich and used without further purification. One side polished silicon wafer (University Wafer, Boston, MA) deposited with titanium (∼250 nm) was prepared by e-beam evaporating titanium (physical vapor deposition). The process was progressed in a home-assembled Evaporator 2000 system equipped with a quartz crystal microbalance to precisely monitor the film thickness and with the cryo-pump to reach the high vacuum ($\sim 10^{-7}-10^{-6}$ Torr). After deposition, the substrates were washed with DI water, dried by a N_2 gun, and stored for further usage. Cysteine-containing peptide, KRWWKWWRRC (Tet213), was synthesized by GenScript Corp. (93.4% purity by HPLC) and had a molecular mass 1590.9 Da.

2.2. Instrumentation. Absolute molecular weights of the polymers were determined by gel permeation chromatography (GPC) on a Waters 2690 separation module fitted with a DAWN EOS multiangle laser light scattering (MALLS) detector from Wyatt Technology Corp (laser wavelength λ = 690 nm) and a refractive index (Optilab DSP) detector from Wyatt Technology Corp operated at λ = 620 nm. Aqueous 0.5 N $NaNO_3$ was used as the mobile phase at a flow rate of 0.8 mL/min. The d*n*/d*c* of PDMA and PAPMA was determined to be 0.17 and 0.16 in 0.5 N $NaNO_3$ solution. The d*n*/d*c* of the copolymers was calculated from the NMR composition data and d*n*/d*c* of individual homopolymers and was used for the calculation of the molecular weight.

Attenuated total reflectance Fourier transform infrared (ATR-FTIR) spectra were recorded using a Thermo-Nicolet Nexus FT-IR spectrometer with a MCT/A liquid nitrogen cooled detector, KBr beam splitter, and MKII Golden Gate Single Reflection ATR accessory (Specac Inc.). Spectra were recorded at 4 cm^{-1} resolution, and 256 scans were collected for each sample. Static water contact angles were determined by dropping a water droplet of 2 μL on the surface before a picture of the droplet was taken using a digital camera (Retiga 1300, Q-imaging Co.). Water contact angles were analyzed using Northern Eclipse software. Five different sites were tested for each sample, and the average value is reported. Dry film thickness on the Ti surface was measured by ellipsometry. The variable-angle spectroscopic ellipsometry (VASE) spectra were collected on an M-2000 V spectroscopic ellipsometer (J.A. Woollam Co. Inc., Lincoln, NE) at 55°, 65°, and 75°, at wavelengths from 370 to 1000 nm with an M-2000 50W quartz tungsten halogen light source. The VASE spectra were then fitted with the multilayer model on the basis of the WVASE32 analysis software, using the optical properties of a generalized Cauchy layer to obtain the "dry" thickness of the brush layer. In the case of the peptide conjugated brushes, a similar method was used as the chemical properties of the peptide conjugated brush are similar to the unmodified brush layer. ^{1}H NMR spectra were recorded on a Bruker Avance 300 MHz NMR spectrometer using D_2O as the solvents. X-ray photoelectron spectroscopy (XPS) was performed using a Leybold LH Max 200 surface analysis system (Leybold, Cologne, Germany) equipped with a Mg Kα source at a power of 200 W. Elements were identified from survey spectra. Prior to XPS analysis, all samples were thoroughly dried in vacuum. Fluorescence emission spectra (350 nm excitation) were collected with a Cary Eclipse fluorimeter using excitation and emission slit bandwidths of 5 nm. Samples were thermostated at 25 °C with a Peltier device.

2.3. Synthesis of Copolymer Brushes. *2.3.1. Initiator Modification.* The initiator modification was carried out in two steps: initial functionalization to generate amine groups and hydroxyl groups followed by modification with 2-chloropropionyl chloride to generate ATRP initiators groups on Ti surface. The pretreatment of Ti deposited silicon wafer (Ti) and the amine modification (Ti-NH_2) were carried by following protocols reported in the literature.[28] Primary amine functionalized Ti surface was further modified using glycidol to generate hydroxyl groups.[29] Ti-NH_2 was treated with glycidol (1 mL) in 20 mL of DMF at 50 °C for 24 h. The hydroxyl-modified surface (Ti-OH) was ultrasonically washed consecutively with DMF, methanol, and water. The modified samples were dried in argon flow and stored under argon.

ATRP-initiator modified surface was generated by treating with 2-chloropropionyl chloride. 2-Chloropropionyl chloride (2.50 g, 19.68 mmol) and triethylamine (2.17 g, 21.40 mmol) were added dropwise to Ti-NH_2 or Ti-OH incubated in DCM (30 mL) at 0 °C over a period of 2 h. The reaction was continued at 0 °C for 4 h and left overnight at room temperature. The modified surfaces were cleaned by ultrasonication in DCM, acetone, methanol, and water consecutively and preserved in argon after dried in vacuum. The dried ATRP initiator modified samples (Ti-NH-Cl and Ti-O-Cl) were characterized using XPS and water contact angle measurements.

2.3.2. Surface-Initiated ATRP of N,N-Dimethylacrylamide and N-(3-Aminopropyl)methacrylamide Hydrochloride. All the polymerizations were conducted in a glovebox filled with argon. For a typical experiment, DMA (0.5 g, 5 mmol) and APMA (0.18 g, 1 mmol) were dissolved in degassed purified water (4.5 mL). This solution was introduced into a $CuCl_2$ (0.5 mg, 3.7×10^{-3} mmol), CuCl (3.7 mg, 3.7×10^{-2} mmol), and HMTETA (22 μL, 8.1×10^{-2} mmol) mixture and then stirred until homogeneous. Titanium plates modified with ATRP initiators (Ti-NH-Cl and Ti-O-Cl) were introduced to the polymerization mixture along with the addition of methyl 2-chloropropionate [4.3 μL (in 10% ethanol solution), 3.7×10^{-3} mmol], and the polymerization was continued at 22 °C for 24 h. The polymerization was stopped by exposing it to air and followed by dilution with water. The resulting copolymer grafted Ti plates were ultrasonicated in water two times (30 min each) and dried in vacuum. The solution polymer formed along with the surface grafted polymer was dialyzed against water for 2 days (1000 MWCO membranes), and the polymer was obtained by lyophilization. The copolymer grafted surface (Ti-Brush) was characterized by water contact angle measurements, XPS, ellipsometry, ATR-FTIR, and atomic force microscopy analyses.

2.3.3. Synthesis of Maleimide Group Immobilized Ti Surface. Ti-Brush was immersed in 0.5 M Et_3N/water solution for 2 h at room temperature and ultrasonicated for 20 min to remove the hydrochloride on primary amine groups in the grafted copolymer layer. The surface was washed with water and ultrasonicated consecutively with water, acetone, and methanol to produce primary amine-functionalized brushes (Ti-Brush-NH_2). The primary amine-functionalized surface treated with 3-maleimidopropionic acid *N*-hydroxysuccinimide in

acetonitrile solution (1 M solution) for 6 h at 22 °C, ultrasonicated consecutively with acetonitrile and acetone, and dried. The maleimide-functionalized surface (Ti-Brush-M) was characterized by ATR-FTIR and ellipsometry.

2.3.4. Reactivity of Maleimide Groups in the Copolymer Brush. Ti-Brush-M synthesized from cleavable initiator modified surface (Ti-O-Cl) was incubated with dansyl cysteine solution (50 mg/mL, sodium phosphate buffer) overnight and then with 2-mercaptoethanol for 1 day to quench the remaining maleimide groups in copolymer brush. Ti slide was ultrasonically rinsed with water and acetone for 2 times consecutively to generate the dansyl groups immobilized Ti surface (Ti-Brush-D). The dansyl group immobilized copolymer brush quantitatively cleaved from the surface by incubating with aqueous NaOH solution (1 M) overnight. The supernatant solution was dialyzed for 2 days against water (1000 MWCO) and freeze-dried. The obtained polymer was reconstituted to 1 mL, and the fluorescence spectra were recorded.

2.3.5. Synthesis of Peptide Conjugated Brushes (Ti-Brush-P). In this set of experiments, we used poly(DMA-*co*-APMA) brushes prepared from noncleavable Ti-N-Cl initiator-modified surface. The maleimide-modified Ti surfaces were incubated with a solution of cysteine-containing peptide Tet213 in 100 mM sodium phosphate buffer (1 mg/mL) (10 mL) overnight followed by excess of 2-mercaptoethanol (0.1 g/mL) for another day. The peptide-immobilized Ti slides were cleaned ultrasonically with water for 2 times (15 min each), and the samples were dried in argon flow. The dried samples were stored under argon and characterized by water contact angle measurements, XPS, ellipsometry, ATR-FTIR, and atomic force microscopy analyses. The dried samples were preserved in refrigerator at −20 °C.

2.4. AFM Morphology and Force Measurements. Atomic force microscopy measurements were performed on a commercially available multimode system with an atomic head of 130 × 130 μm^2 scan range which used a NanoScope IIIa controller (Digital Instruments, Santa Barbara, CA). Surface morphology was examined under PBS buffer in contact mode using a commercially manufactured V-shaped silicon nitride (Si_3N_4) cantilever with gold on the back for laser beam reflection (Veeco, NP-S20). The spring constant of the AFM cantilever was measured using the thermal equipartition theorem.[30,31] Force measurements were performed in PBS buffer. On tip approach the onset of the region of constant compliance was used to determine the zero distance, and on retraction the region in which force was unchanged was used to determine the zero force. The rate of tip−sample approach or retraction was typically 0.5 μm/s.

The raw AFM force data (cantilever deflection vs displacement data) were converted into force vs separation following the principle of Ducker et al. by using custom Matlab v.5.3 (Math Works, Natick, MA) software.[32] The software converts the cantilever deflection vs linear voltage displacement transformer signal into restoring force vs tip−substrate separation using user input trigger and spring constant values. We followed our published protocol for the calculation of the adhesive force.[33] Average value ± SD from 50 different force curves from different spots on the substrate are reported.

2.5. A Model for the Analysis of Peptide Grafting to Polymer Brushes from the Thickness Measurements. The brush height (h) on a flat surface is related to the molecular weight M_n and the graft density (σ) of the chains as defined by the following equation[35]

$$h = \frac{\sigma}{\rho N_A} M_n \quad (1)$$

where ρ is the density of the polymer layer and N_A is the Avogadro number. At constant graft density and density of the polymer layer, eq 1 can be written as

$$h = cM_n \quad (2)$$

where c is also a constant. The postmodification of brush layer with maleimide and peptide will result in an increase in the molecular weight of the grafted chains with a proportional increase in dry thickness of the polymer film on the surface (Figure 1). The increase

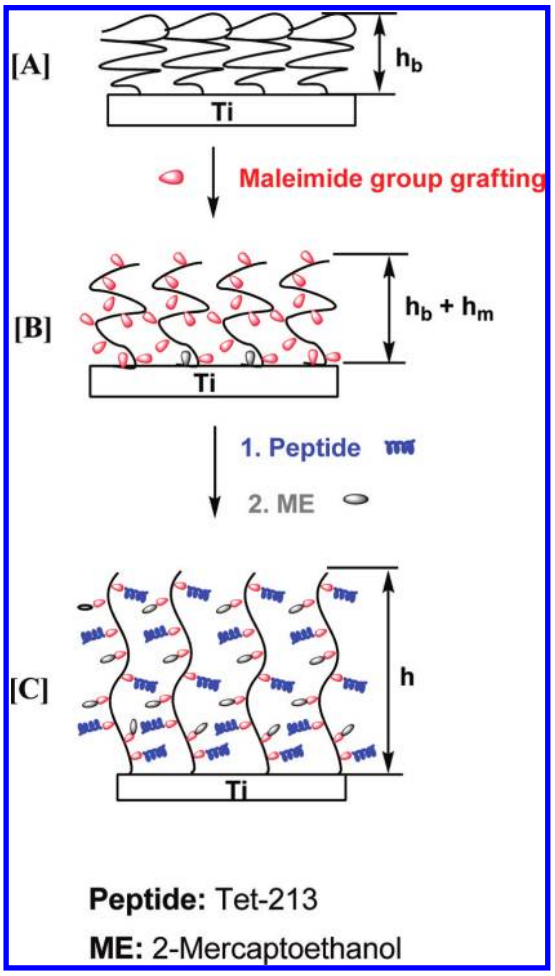

Figure 1. Model for the calculation of thickness increase after the modification of copolymer brushes on Ti surface. [A] Ti substrate grafted with copolymer brush. [B] Thickness increase after the conjugation of maleimide linker. [C] Thickness increase after peptide conjugation followed by 2-mercaptoethanol quenching.

in the thickness of the polymer film was used for the calculation of the amount of peptide conjugated to the polymer brush. This is based on following assumptions:[35,36] (i) the optical properties and density of the polymer layer before and after modification remained constant, (ii) the graft density of the brush layer remained constant before and after conjugation for a given sample, and (iii) the peptide grafted film is uniform. In the present case, the grafted chains and subsequent modifications (maleimide or peptide conjugation) resulted in similar chemical structures so that the optical properties and density of the modified layer can be considered similar to the original polymer layer. Based on this, similar fitting parameters were used for the estimation of dry thickness by ellipsometric measurements before and after maleimide or peptide conjugation. The dry thickness was also confirmed by AFM scratch analysis. Since the molecular weights of the grafted chains before maleimide or peptide conjugation were known, the increase in molecular weight was estimated from the increase in thickness and was used for the calculation of peptide density.

The change in dry thickness can be written as (detailed analysis is given in Supporting Information)

$$\Delta h = c\Delta M_n \quad (3)$$

where Δh is the change in thickness, c is a constant, and ΔM_n is the change in molecular weight. Equation 4 was deduced from eq 3 to determine the molecular weight increase after peptide

Scheme 1

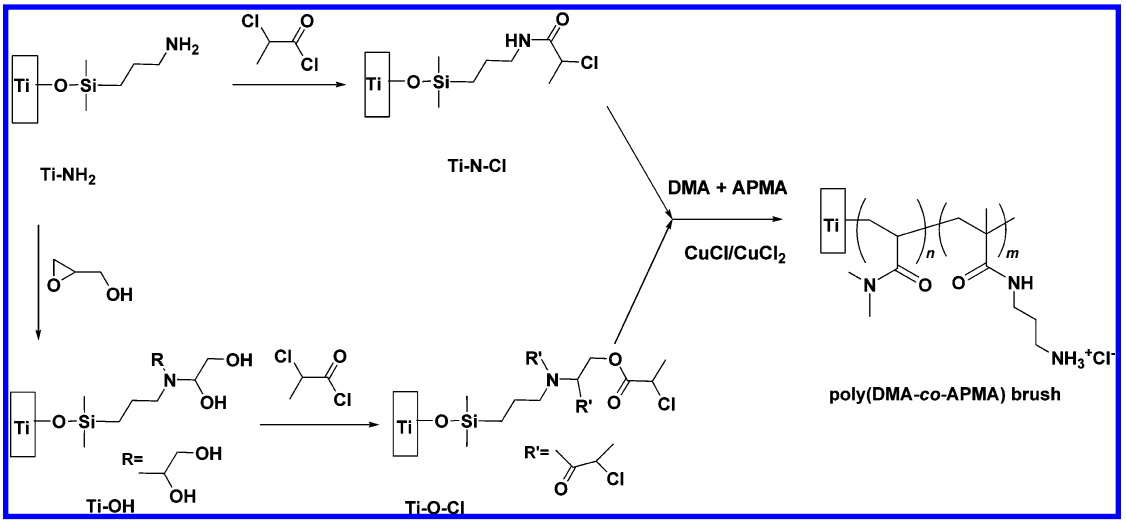

conjugation to brushes

$$h - h_b = c(\Delta M_{nm} + \Delta M_{np} + \Delta M_{nE}) \quad (4)$$

where ΔM_{nm} is the molecular weight increase after maleimide coating, $\Delta M_{np}$the molecular weight increase after peptide coating, ΔM_{nE} the molecular weight increase after 2-mercaptoethanol coupling, h the brush thickness after peptide conjugation, h_b the brush thickness before conjugation, and c the linear constant (see Supporting Information for more details). Similar analyses for the postmodification of polymer grafted layers were reported recently.[35,36]

2.6. Antimicrobial Activity of Peptide-Immobilized Ti Slides. The peptide-immobilized surfaces were washed several times with 0.1 M EDTA sodium salt solution and then with water to remove any traces of copper ions present before preparing for antimicrobial studies. Peptide-immobilized polymer brush-coated and bare Ti slides were each placed in a well of a 24-well microtiter plate. The samples were then sterilized with 300 μL of 70% ethanol for 5 min. The ethanol solution was subsequently removed after every 5 min, and the sterilization was repeated 5 times. The samples were then equilibrated 5 times with 300 μL of 1X BM2 culture media. 200 μL of *Pseudomonas aeruginosa* (*P. aeruginosa*) PA01 expressing a luciferase gene cassette (*luxCDABE*) was added to each well that contained a titanium sample to get a final concentration of $(1-5) \times 10^5$ CFU/mL. This enables for bacterial quantification using luminescence. The microtiter plate was then placed on a shaker at the speed of 190 rpm to provide a homogeneous liquid environment for the interaction. Incubation was done at 37 °C for 4 h. The bacterial culture without Ti plate was then transferred to a 96-well TECAN plate, and the luminescence emission was measured using a TECAN Spectrafluor Plus spectrometer (TECAN U.S., Inc.). A decrease in the luminescence reading is directly related to the inhibition of the bacterial growth which has previously been confirmed by bacteria colony count (CFU) measurements.[23−25]

The luminescence inhibition of the examined sample was calculated by the equation

$$R_p = \frac{I_c - I_p}{I_c} \times 100\% \quad (5)$$

where R_p is the inhibition of luminescence, I_c the average luminescence of control sample (pure Ti slide), and I_p the average luminescence of peptide-immobilized Ti slide.

3. RESULTS AND DISCUSSION

3.1. Surface-Initiated Copolymerization of DMA and APMA. Reactions involved in the synthesis of the copolymer brushes are given in Schemes 1 and 2. Primary amine groups were generated on Ti surfaces (Scheme 1) by silanization using APTES. The modification resulted in a layer thickness of ~5 nm suggest that a multilayer was formed in this case and was consistent with literature reports on Ti surface modification[28] using APTES. The experimental conditions were optimized to limit the polymerization of APTES and ensure the stability of this layer on Ti surface. After the initial amine modification we performed either (i) a reaction with 2-chloropropionyl chloride to generate an amide functionalized noncleavable initiator layer (Ti-N-Cl) or (ii) a reaction with glycidol followed by the reaction with 2-chloropropionyl chloride to generate an ester linker cleavable initiator layer (Ti-O-Cl) on the titanium surface. Detailed characterization of these surfaces is given in section 3.4.

The initiator-modified surfaces were used for the surface-initiated polymerization. To generate functional polymer grafted layers, DMA and APMA were copolymerized by aqueous surface-initiated ATRP from the Ti surface at room temperature.[29,33] The monomer feed ratio and the reaction time were changed to generate copolymer brushes with different compositions and graft densities (Table 1). The graft densities of the polymer grafted layer were calculated using following eq 1. The density of the copolymer used was (1.20 g/mL), and h was the polymer layer thickness measured by ellipsometry analysis. Since it was very difficult to obtain sufficient cleaved polymer from the flat Ti surface (due to the limited surface area) for unambiguous determination of molecular weight by GPC, the molecular weight and PDI of the grafted chains obtained were taken as equal to that of the soluble polymer formed along with the surface grafted polymer for calculations. Although this is not an ideal case, the assumption is based on the reported evidence that the molecular weights of the grafted chains are similar in most cases as the soluble polymer formed along with the grafted chains;[10,29,33,34,37,38] however, exceptions are reported. Based on the current brush literature, this may not produce large error in the estimation of graft density.[10,29]

The characteristics of the copolymer brushes are given in Table 1. Irrespective of the monomer feed ratio, the graft density of the chains increased with the reaction time. Longer polymerization time resulted in high graft density compared to the shorter polymerization time. The molecular weight of the

Table 1. Effect of Reaction Time and Monomer Feed Ratio on Poly(DMA-*co*-APMA) Grafting on Ti Surface[a]

sample	time[e] (h)	$[DMA]_0/[APMA]_0$	M_n ($\times 10^{-4}$)[b]	M_w/M_n[b]	dry thickness, h_b[c] (nm)	graft density[d] (chains/nm^2)
Ti-14C	2	5/1	17.03	1.33	15.6 ± 2	0.068
Ti-15C	6	5/1	17.32	1.41	23.8 ± 2	0.10
Ti-16C	8	5/1	16.96	1.51	26.6 ± 1	0.113
Ti-4C	24	5/1	13.93	1.47	30.9 ± 1	0.16
Ti-17C	88	5/1	15.85	1.45	42.5 ± 2	0.196
Ti-18C	3	4/1	18.21	1.21	9.4 ± 2	0.038
Ti-19C	5	4/1	17.10	1.26	17.9 ± 2	0.076
Ti-20C	7	4/1	19.22	1.31	25.3 ± 1	0.096
Ti-21C	16	4/1	19.97	1.38	33.2 ± 4	0.121
Ti-22C	24	4/1	16.71	1.49	35.8 ± 1	0.157
Ti-23C	3	3/1	17.33	1.15	7.9 ± 2	0.033
Ti-24C	5	3/1	16.79	1.17	20.8 ± 2	0.09
Ti-25C	7	3/1	18.98	1.13	31.2 ± 1	0.12
Ti-26C	16	3/1	19.12	1.19	32.5 ± 3	0.123
Ti-27C	24	3/1	14.86	1.29	34.2 ± 2	0.168

[a]Conditions: $[HMTETA]_0/[CuCl]_0/[CuCl_2]_0/[I]_0/[DMA]_0/[APMA]_0$ = 2.2/1/0.1/0.1/130/26, $[DMA]_0$ = 1 mol/L, 22 °C. Grafted polymer layers were synthesized from Ti-N-Cl (noncleavable initiator modified surface). [b]Determined by GPC. [c]Determined by ellipsometry. [d]Calculated from brush thickness and M_n. [e]Polymerization time.

Scheme 2

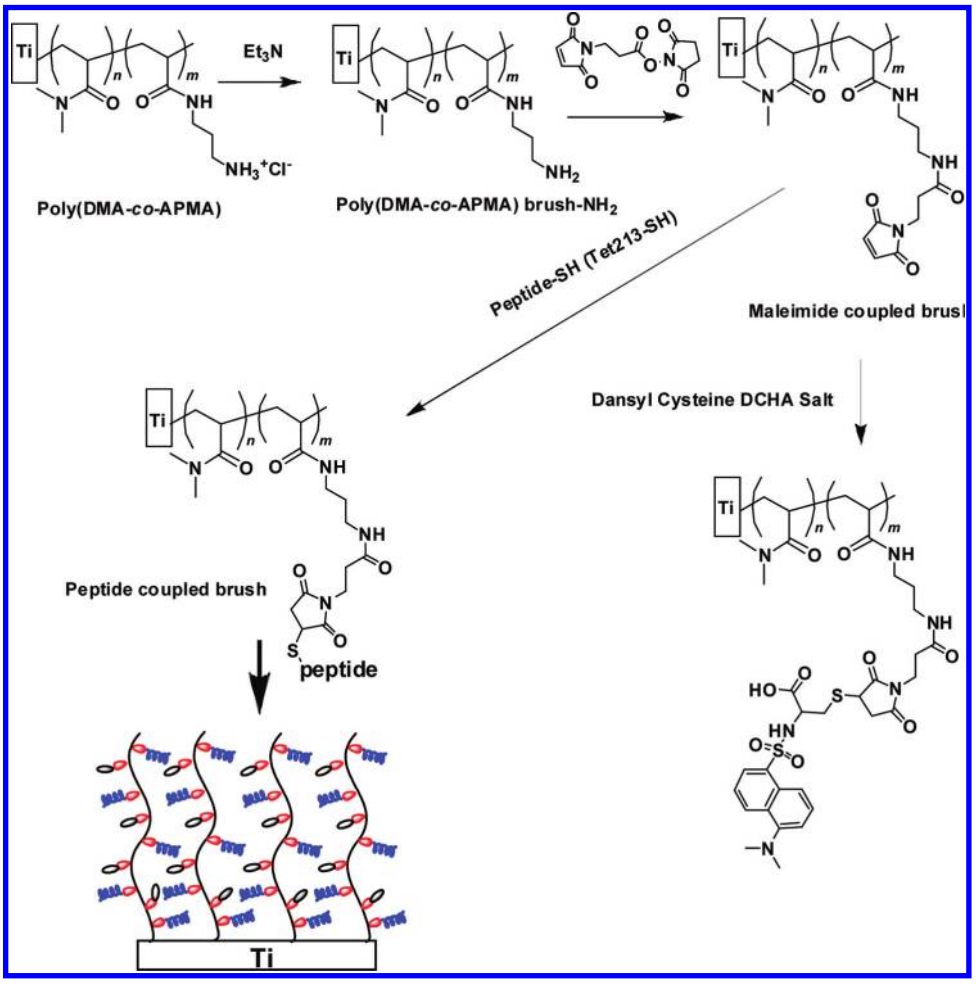

chains remained almost constant with increase in polydispersity of the chains. We believe this is due to the slow initiation from the surface and very high polymerization rate of acrylamide-based monomers (DMA and APMA in this case) in aqueous ATRP conditions. Similar observations were previously made for the aqueous surface-initiated ATRP of acrylamide-based monomers,[29,33,37,39,40] suggesting that more polymer chains were added to the grafted layer with time. The increase in the dry thickness of the grafted layer with time at relatively constant molecular weight is reflective of increase in the graft density.[29,33,37,40] Previously, we have unambiguously demonstrated this in the case of aqueous ATRP of DMA from PVC

dx.doi.org/10.1021/bm2009697|*Biomacromolecules* 2011, 12, 3715–3727

surface by cleaving and analyzing the grafted PDMA chains grown on the surface.[29] The grafted chains have similar properties of soluble polymer chains formed in solution. We anticipate a similar behavior here for the copolymerization of DMA and APMA as these are acrylamide-based monomers. We also acknowledge the fact that the polymerization was not an ideal controlled ATRP polymerization. A GPC trace of polymer obtained from the sample Ti-4C (Table 1) presented in Figure 5S (Supporting Information) showed a monomodal distribution of the polymer chains. Since the molecular weight of the chains remained almost constant with reaction time, this provided an alternate way to make copolymer grafted layers with difference in graft density without having considerable effects on the molecular weight. The graft density of each PDMA-*co*-PAPMA grafted sample reported was calculated from the independent measurements of molecular weight of soluble polymer formed along with the grafted layer, dry thickness measured by the ellipsometry, and the density of the polymer. Thus, we are confident about the graft density values given in Table 1 and its subsequent use in the interpretation of peptide conjugation and antimicrobial activity in the following sections (sections 3.6 and 3.7).

The monomer feed ratio did not significantly affect the molecular weight of the polymer grafts. The PDI of copolymer chains decreased with a decrease in $[DMA]_0/[APMA]_0$ feed ratio. The presence of APMA might have prevented the rapid growth of polymer chains and giving low polydispersity of chains. Another factor which might have influenced the polymerization was the presence of hydrochloride on the APMA which could possibly poison the ATRP catalyst resulting in a change in polymerization kinetics. The soluble copolymers formed along with grafted chains were analyzed by ^{1}H NMR, and the results showed that the copolymer compositions are similar to those of the initial monomer feed ratios (Figure 4SB in Supporting Information). The polymer layer formed on the Ti surface was quite stable in aqueous conditions for several months even though the initial APTES modification was a multilayer (5 nm thickness) as evident from the measured dry thickness of the polymer film by ellipsometry at different time intervals (data not shown).

3.2. Reactivity of the Amine Groups in the Copolymer Brushes. After the DMA/APMA copolymer grafted layers were successfully synthesized and characterized, we studied the reactivity of the primary amine groups within the grafted layer. This is required in part to assess and control the modification processes as described in Scheme 2. The primary amine groups on the copolymer brushes were regenerated by treating them with triethylamine and subsequently reacted with 3-maleimidopropionic acid *N*-hydroxysuccinimide ester to generate maleimide-functionalized copolymer brushes on Ti surfaces (Scheme 2). The maleimide groups were further reacted with fluorescent dansyl cysteine by a Michael-type addition between maleimide and thiol groups. The presence of dansyl groups in the brush was assessed after cleavage of the copolymer grafts from the Ti surface. We used grafted copolymer layer synthesized from ester linked initiator modified surface (Ti-O-Cl). The fluorescence spectrum (Figure 1S, Supporting Information) of the cleaved grafts indicated the efficient conjugation of dansyl groups to the grafted chains. This result demonstrated the reactivity of the primary amine groups within the copolymer brush. The proton NMR spectra of the soluble polymer grafted with maleimide group (peak at 6.78 ppm) (Figure 6S, Supporting Information) also demonstrated the conjugation, and primary amine groups were quantitatively converted to maleimide groups. The number of dansyl groups on the polymer grafts was not calculated due to the nonquantitative nature of the fluorescence emission.

3.3. Peptide Conjugation to Copolymer Brushes. The conjugation scheme detailing the immobilization of the cysteine end-functionalized AMP (Tet-213) onto copolymer brushes on Ti surfaces is given in Scheme 2. Polymer grafted layers prepared from noncleavable Ti-N-Cl initiator layer was used in these experiments. Several variations of copolymer brushes were used for the peptide conjugation (Table 2). The peptide conjugated surfaces were characterized by XPS, ellipsometry, AFM, and contact angle measurements; details are given in the following section.

Table 2. Characteristic of Peptide Conjugated Poly(DMA-*co*-APMA) Brushes on Ti Surface[a]

sample[b]	dry thickness increase[e] (nm)	amine saturation, r_p (peptides/amine)[c] (%)	mass of peptides W_p[d] (μg/cm^2)
Ti-14C-P	28.6 ± 4	69 ± 11	3.1 ± 0.5
Ti-15C-P	32.8 ± 4	49 ± 6	3.4 ± 0.4
Ti-16C-P	36.2 ± 1	48 ± 1	3.7 ± 0.1
Ti-4C-P	39.2 ± 2	44 ± 2	3.8 ± 0.2
Ti-17C-P	44.0 ± 3	33 ± 2	3.9 ± 0.2
Ti-18C-P	19.3 ± 5	65 ± 16	2.1 ± 0.5
Ti-19C-P	37.0 ± 6	66 ± 11	3.8 ± 0.6
Ti-20C-P	44.5 ± 2	54 ± 3	4.6 ± 0.3
Ti-21C-P	42.1 ± 6	35 ± 5	3.8 ± 0.5
Ti-22C-P	32.6 ± 2	22 ± 1	2.6 ± 0.1
Ti-23C-P	15.6 ± 3	49 ± 10	1.6 ± 0.3
Ti-24C-P	40.4 ± 4	48 ± 5	4.0 ± 0.4
Ti-25C-P	44.1 ± 2	32 ± 1	4.0 ± 0.1
Ti-26C-P	42.7 ± 5	28 ± 3	3.6 ± 0.4
Ti-27C-P	34.7 ± 2	19 ± 1	2.6 ± 0.1

[a]Condition: peptide: Tet-213. [b]Peptide-coated Ti samples by corresponding copolymer brush with sample code without "P" given in Table 1. [c]Calculated by eq 7S in Supporting Information. [d]Calculated using eq 11S in Supporting Information. [e]The value of the dry thickness increase is after peptide conjugation and mercaptoethanol quenching.

3.4. Surface Characterization. *3.4.1. Contact Angle Measurements.* Table 3 shows the air−water contact angles on Ti surface at different stages of modification. Amine modification resulted in an increase in the hydrophobic character of the surface as evidenced by an increase in contact angle from 19° (Ti-) to 69° (Ti-NH_2). Reaction of chloropropionyl chloride resulted in an increase in water contact angle, suggesting that that the amine groups were modified. In the case of glycidol modification of amine groups, the contact angle decrease was due to the formation of hydroxyl groups. Subsequent reaction with chloropropionyl chloride generated a more hydrophobic surface due to the formation of hydrophobic chloropropionate groups on the surface. The change in the water contact angle of the surface was directly related to the modifications as shown in Schemes 1 and 2. The copolymer brush was relatively hydrophilic compared to the initiator-modified surface. The peptide conjugation resulted in an increase in hydrophobic character of the surface due to the amphiphilic nature of the peptide Tet213.

3.4.2. X-ray Photoelectron Spectroscopy (XPS) and ATR-FTIR Analysis. Figure 2S (Supporting Information) shows the X-ray photoelectron spectra of amine-modified titanium, poly(DMA-*co*-APMA) (5/1), and Tet213-modified poly-(DMA-*co*-APMA) copolymer brush. Good correlation of

Table 3. Water Contact Angle and Experimental Molar Ratio of C/N, C/Cl, C/O, and Cl/N Obtained from the XPS Survey Scan and Theoretical Value Calculated Based on the Molecular Structure

samples	contact angle (deg)	surface composition from XPS analysis[c]				
			C/N	C/Cl	C/O	Cl/N
Ti-NH_2[b]	69.0 ± 1.1	theoretical	5	N/A	N/A	0
		experimental	9	50.6	1.5	0.18
Ti-N-Cl	85.6 ± 1.5	theoretical	8	8	8	1
		experimental	10.6	15	1.7	0.7
Ti-PDMA-*co*-PAPMA[a]	42.1 ± 1.3	theoretical	4.6	32	5.3	0.14
		experimental	5.6	32.8	5.6	0.17
Ti-PDMA-*co*-PAPMA-Tet213[a]	65.4 ± 1.7	theoretical	3.7	N/A	4.5	0
		experimental	5.9	N/A	5.5	0
Ti-OH	46.8 ± 1.0		ND	ND	ND	ND
Ti-O-Cl	91.1 ± 1.2		ND	ND	ND	ND

[a]For samples Ti-4C and Ti-4C-P, respectively (Tables 1 and 2); ND = not determined. [b]Contact angle of Ti surface before modification was 19°. [c]Theoretical elemental composition was calculated from the chemical structure. In the case of Ti-PDMA-*co*-PAPMA, the monomer feed ratio is used for this estimation. In the case of peptide conjugated brushes, the copolymer composition and peptide density were used.

experimental molar ratios C/O, C/N, and C/Cl, with the theoretical values for the surface, indicated the formation of poly(DMA-*co*-APMA) copolymer brush and the desired modifications. Upon Tet213 conjugation, the Cl 2p peak disappeared with the appearance of a characteristic presence of nitrogen, carbon, and oxygen. The ratio of elemental composition of the surfaces as measured by XPS (Table 3) also confirmed the required surface modification. Since there is overlap between the amide nitrogen and carbonyl groups of PDMA, APMPA, and the peptide Tet213, we have not attempted to calculate the peptide density from XPS measurements.

Figure 3S shows a representative ATR-FTIR spectrum of Tet213 conjugated to copolymer brush on Ti surface. The presence of a characteristic amide I absorption (1701 cm^{-1}) along with other peaks of Tet213 in the ATR-FTIR spectrum of the peptide conjugated copolymer brush, demonstrated the effective peptide conjugation. There was a slight shift in the amide I peak position of surface grafted Tet213 compared to pure Tet213. The attachment of peptides to copolymer brush was also evident from the dramatic increase in the brush thickness as measured by AFM and ellipsometry. The increase in brush thickness upon peptide conjugation may not be due to the surface aggregation of the peptides as the peptide grafted surface was extensively cleaned by sonication in good solvent for both the copolymer and the peptide before the measurements, suggesting covalent attachment.

3.5. Analysis of Peptide Grafting to Polymer Brushes. On the basis of the model described in the experimental section 2.5, the amounts of peptide conjugated to different polymer brush samples were calculated. Calculations using ellipsometric thickness measurements are exemplified for the peptide conjugated copolymer brush sample Ti-4C-P (Tables 1 and 2). The dry thickness of the original polymer layer was 30.9 ± 1.1 nm, and the molecular weight and PDI of the chains were 139.3 kDa and 1.47, respectively. Upon conjugation with 3-maleimidopropionic acid *N*-hydroxysuccinimide ester, the thickness of the brush increased to 36.0 ± 1.3 nm, suggesting a quantitative conversion of amine groups to maleimide groups indicating a >97% conversion. Upon conjugation of peptide (Tet213) and mercaptoethanol quenching the thickness increased to 70.1 ± 1.4 nm. The estimated peptide saturation (or the percentage of APMA groups with peptide) on the grafted chains was ~44% of maleimide groups (Table 2) which is equal to 90 ± 4 peptides/chain corresponds to 3.8 ± 0.2 $\mu g/cm^2$. The dry thickness of the copolymer brush and peptide conjugated sample were confirmed using AFM scratch analysis, suggesting that ellipsometric thickness measurements can be used for the estimation of peptide density on the surface. Following the same principles, we calculated the peptide surface density and peptides/chain for the other peptide conjugated brushes (Table 2). The maleimide conjugation to brushes resulted in almost quantitative conversion in every case as evident from the increased dry thickness.

3.6. Effect of Copolymer Composition and Graft Density of Brushes on Peptide Conjugation. Figure 2 shows the influence of graft composition of copolymer brush on the number of peptides per polymer chain at three different graft densities. Even though the number of amine groups and maleimide groups per polymer chain increased from 20 to 33 mol % with increasing APMA content of the brush, the number of Tet213 molecules conjugated per polymer chain did not show marked differences at similar graft densities. There was a dramatic decrease in the number of peptides grafted per polymer chain with increase in graft density (number of

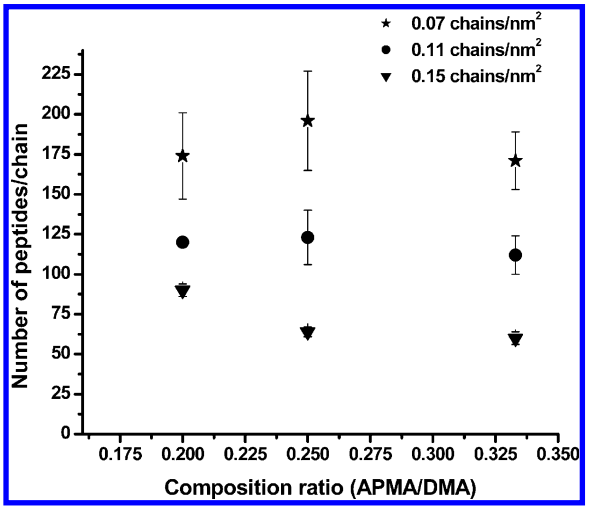

Figure 2. Effect of graft density and composition on the number of peptides grafted onto poly(DMA-*co*-APMA) brush. Tet213 is used for the conjugation. The composition ratio is given for APMA/DMA: 1/5, 1/4, and 1/3.

dx.doi.org/10.1021/bm2009697|*Biomacromolecules* 2011, 12, 3715–3727

peptides/polymer chain) of the copolymer brush. More than 200 peptides per polymer chain were grafted in some cases. These results showed that the number of reactive functionalities (i.e., composition) within the copolymer brush was not the major contributing factor influencing the number of peptides grafted per chain as opposed to graft density of chains on the surface.

The influence of the graft density of the copolymer brush on peptide conjugation is further exemplified by the data given in Figure 3. The number of peptides grafted per chain and peptide density (peptides/nm^2) on the surface were plotted against the graft densities of copolymer brushes at different compositions. The number of peptides grafted per polymer chain decreased with increase in grafting density for all the three polymer compositions studied. The decrease in the number of peptides grafted with increase in graft density may be due to the steric restrictions imposed by the close grafting of polymer chains and decrease in interchain distance. This might have restricted the diffusion of peptides to the interior of the copolymer brush layer. Since the maleimide reaction was quantitative (as evident from the ellipsometry thickness analysis and fluorescence measurements), this is possibly due to the large size of the peptide compared to the 3-maleimidopropionic acid *N*-hydroxysuccinimide ester or dansylcysteine groups. Based on the ellipsometric analysis, more than 97% of amine groups were converted to maleimide group within the copolymer brush but the fraction of peptide attached APMA units (amine saturation) decreased with increasing graft density (Table 2). It varied from 19 to 69%. This supports the influence of steric factor on peptide conjugation to polymer brushes.

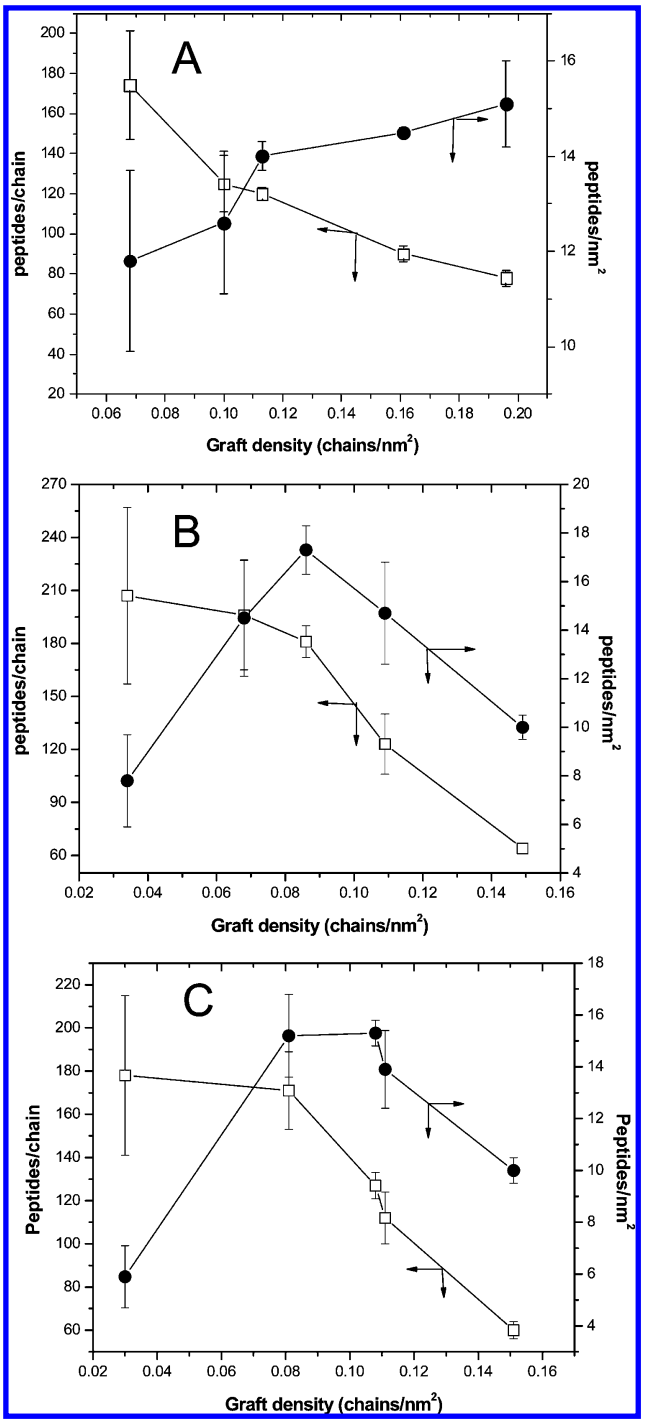

Figure 3. Effect of graft density on number of peptides grafted per chain and peptide density on the surface: (A) 5/1 (DMA/APMA); (B) 4/1 (DMA/APMA); (C) 3/1 (DMA/APMA).

When the peptide density on the surface (peptide/nm^2) was plotted against graft density, the dependence on graft density was different for various copolymer compositions. The peptide surface density increased with increasing graft density up to a medium graft density for all copolymer compositions. However, in the case of the composition DMA/APMA (5/1), the peptide density increased with increasing graft density. Since the maleimide conjugation was quantitative, the observed behavior was due to the peptide conjugation as well the difference in the distribution of reactive groups within the brush structure. In the case of copolymer compositions 4/1 and 3/1 (DMA/APMA), the peptide surface density decreased at high graft densities after reaching a maximum. The peptide density values reached as high as 17 peptides/nm^2 with values ranging from 10 to 17 peptides/nm^2, which is considerably higher than the density observed after direct surface conjugation of peptide onto Ti surfaces (1 to 4 peptide/nm^2).[41] Our data demonstrate that a range of peptide density on the surface can be generated by changing the brush properties.

Since the peptide surface density was getting saturated at higher graft densities, it is apparent that there was some nonuniformity in the peptide conjugation with graft density on a vertical scale. If there was a uniform peptide conjugation along the grafted chain, one could anticipate a near linear increase in peptide density with increase in graft density. However, in our case, only at composition 5/1 DMA/APMA of the brush a close linearity was observed. We propose that majority of the peptides might be coupling near to the surface at high graft densities since diffusion of peptides to the interior of the brush layer is restricted due to relatively large size of the peptide and close grafting of polymer chains. The increase in peptide/nm^2 on the surface with increase in graft density was due to the increase in the number of polymer chains per unit area even though the peptides/chain was decreasing. Since we do not have experimental data on the distribution of peptides along the height (vertical scale) of the brushes, it is difficult to confirm these arguments.

3.7. Antimicrobial Properties. It has been suggested that the soluble antimicrobial peptides (AMPs) adopt well-defined structures upon interaction with bacterial membranes and these structural change are directly related to their antimicrobial functions.[42] In the case of surface tethered AMPs, it has been postulated that the disturbance of surface electrostatics at the

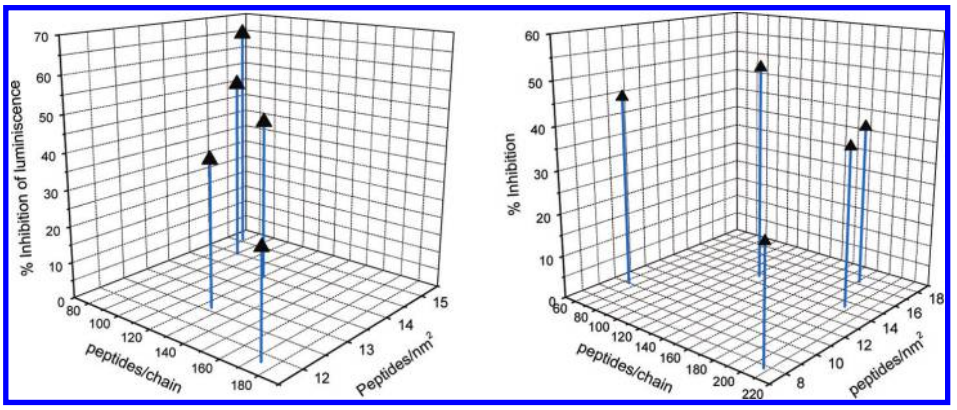

Figure 4. Effect of peptide density on the bacterial inhibition at 5/1 (DMA/APMA) composition of the peptides. Error estimation for the % inhibition was ±5.

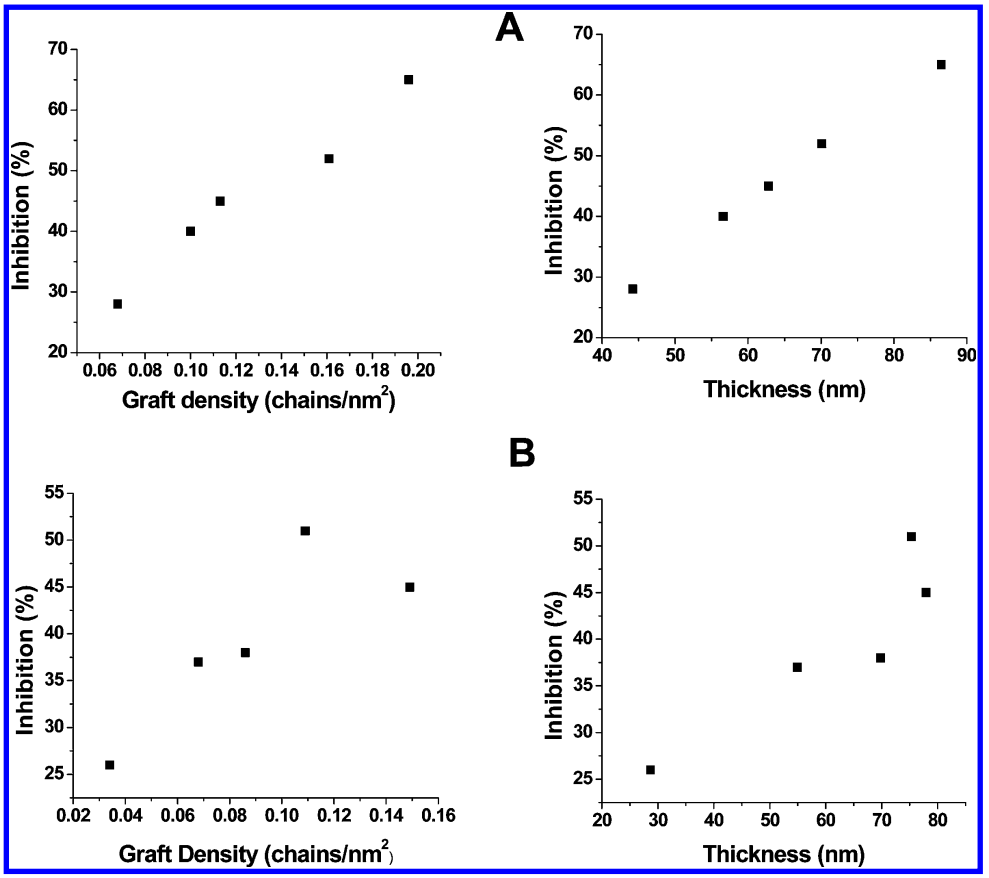

Figure 5. Effect of graft density and thickness of the peptide grafted brush on bacterial growth inhibition. Compositions (DMA/APMA) 5/1 (A) and 4/1 (B) are shown. Error estimation for the % inhibition of luminescence was ±5.

bacterial surface upon interaction with tethered peptides may trigger an autolytic and/or cell death mechanism.[24,43,44] This is the reason for their antimicrobial properties and tethered peptides can possibly kill several bacteria. Thus, the high charge density on the surface associated with the peptide conjugation to brushes, the flexibility of the polymer brush linker, and conformational restrictions of polymer chains in the brush (graft density and steric factors) are all may contribute to antimicrobial activity of polymer brush conjugated AMPs. Thus, we investigated the influence of brush properties on antimicrobial activity of the peptide conjugated surface.

Figures 4 and 5 show the influence of polymer brush properties and the number of peptides grafted on the antimicrobial activity of the surface. The antimicrobial activity of the surface is reported as inhibition of luminescence by *Pseudomonas aeruginosa* (*P. aeruginosa*) PA01 expressing a luciferase gene cassette (*luxCDABE*). A decrease in the luminescence reading was directly related to the inhibition of the bacterial growth which has previously been confirmed by bacteria colony count (CFU) measurements.[23−25] The control samples Ti-surface and Ti-PDMA and Ti-PDMA-*co*-APMA did not show any inhibition of the luminescence, suggesting that they were not bactericidal. Figure 4 shows the influence of number of peptides/chain and peptide surface density on the antimicrobial activity of the surface at two different copolymer compositions (5/1 and 4/1 DMA/APMA). In general, the

dx.doi.org/10.1021/bm2009697|*Biomacromolecules* 2011, 12, 3715−3727

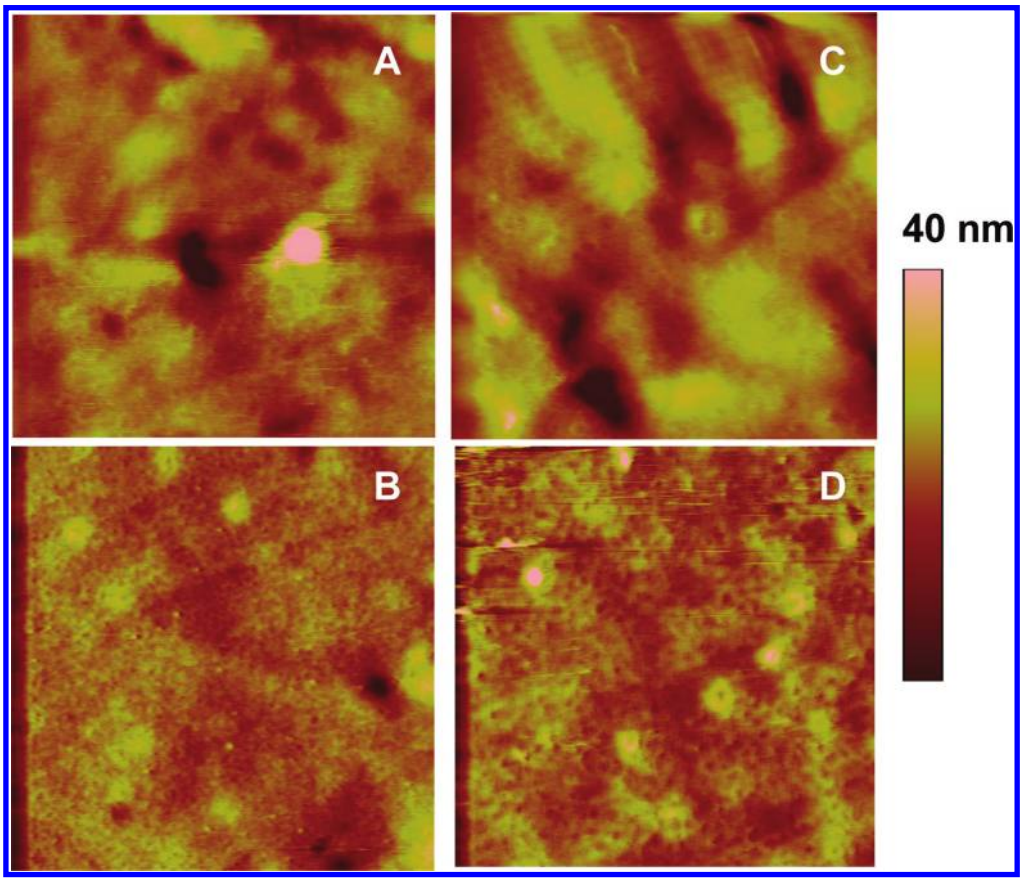

Figure 6. Surface morphology of (A) poly(DMA-*co*-APMA) brush (sample Ti-4C), (B) Tet213 conjugated poly(DMA-*co*-APMA) brush (Ti-4C-P-high graft density), (C) poly(DMA-*co*-APMA) brush (sample Ti-14C), and (D) Tet213 conjugated poly(DMA-*co*-APMA) brush (Ti-14C-P-low graft density). The scan size is 4 μm × 4 μm.

antimicrobial activity was higher for surfaces with higher peptide surface density. Although the number of peptides grafted per chain was lower in these cases, the average peptide surface density was higher. Copolymer composition did not have a huge influence as similar antimicrobial activities were obtained for both compositions studied. The influence of the peptide density (peptides/nm^2) was more evident in the case of the 4/1 composition; higher peptide density gave higher antimicrobial activity (at similar peptides/chain).

We also investigated the influences of graft density and thickness of the peptide conjugated brushes on the antimicrobial activity (Figure 5). Generally, high graft density and thickness resulted in increased antimicrobial activity of the surface. The effect was more pronounced in the case of 5/1 composition than 4/1 composition. This may be due to the lower peptide density at high graft density in the case of 4/1 DMA/APMA composition (see Figure 3B). The enhanced antimicrobial activity with increases in graft density also suggest that, in combination with peptide surface density, the conformation of the grafted chains may also be influencing the antimicrobial activity of polymer brush immobilized peptides (Figure 5A). This is due the fact that at low graft densities not all peptides might be exposed to the outer surface due to the large conformational freedom of the chains. This might allow the self-assembly of the amphiliphilic AMPs within the brush layer which might prevent their interactions with bacterial membrane. But as the graft density became higher, such associations could be limited due to the conformational restrictions of closely grafted chains. The peptides will have better interactions with bacterial membrane and will be more bactericidal. With increase in graft density, the brush thickness (brush thickness after peptide grafting) also increased (Tables 1 and 2). A similar correlation can be found with increase in brush thickness (Figure 5B). Thus, the enhanced antimicrobial activity at high graft densities of the copolymer brush was due to a combination of limited chain flexibility, higher thickness, and high peptide density on the surface. Thus, our results strongly suggest that the optimization of peptide density and graft density (related conformational flexibility) were critical in obtaining highly effective antimicrobial coatings.

3.8. Surface Analysis by Atomic Force Microscopy.

The morphology and hydrophilic/hydrophobic character of the surface were known to be important parameters for the adhesion of bacteria and biofilm formation.[2,8] We have previously shown that the initial adhesion of bacteria to the surface depends on the hydrophobic character of the surface.[25] Since hydrophilic polymer brushes are nonadhesive in nature,[33] we investigated their properties after peptide conjugation. We also wanted to investigate the uniformity of the surface as well as changes in surface features after peptide conjugation by measuring the surface morphology.

Figure 6 shows the surface morphologies of poly(DMA-*co*-APMA) brush and Tet213 grafted poly(DMA-*co*-APMA) brush at two different graft densities (0.068 and 0.161 chains/nm^2). Similar morphologies were observed for brushes before peptide conjugation and the surface roughness measurements were 6.1 and 5.8 nm, respectively, for low and high graft density brushes. The AFM images of peptide conjugated brushes showed

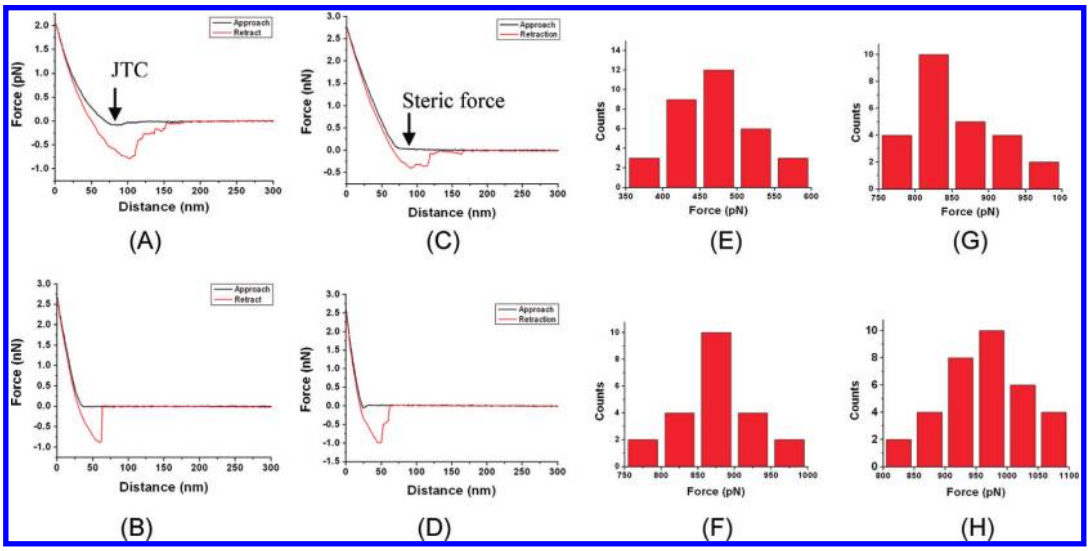

Figure 7. Representative approach (black line) and retraction (red line) force curves for samples Ti-14C (A), Ti-4C (C), Ti-14C-P (B), and Ti-4C-P (D) and probability distribution histograms of the maximum adhesive force upon retraction for samples Ti-4C (E) and Ti-4C-P (F). Probability distribution histograms of the maximum adhesive force during retraction for samples Ti-14C (G) and Ti-14C-P (H). Details of the samples are given in Tables 1 and 2. Ti-4C is high graft density brush, and Ti-14C is low graft density brush.

different features (Figure 6B,D). Importantly, the surface features were regular suggest a uniform grafting of polymer chains and peptides on the surface.

The representative AFM force curve for the sample Ti-14C (0.068 chains/nm^2) is shown in Figure 7A. A weak jump-to-contact (JTC) force ~75 pN was observed when the AFM tip approached the surface. During retraction, or pull-off, a much stronger adhesive force 840 ± 22.3 pN was observed. Probability distribution histograms of the maximum adhesive force for sample Ti-14C are shown in Figure 7G. The strong adhesive force was due to the hydrophobic interaction between the AFM tips and the polymer chains. Figures 7C and 7E show the representative force curves and probability distribution histograms of the maximum adhesive force, respectively, for sample Ti-4C (high graft density brush). The JTC force was not observed on the approach curve; instead, there was a weak steric repulsion. This was due to the higher graft density of the polymer layer. The maximum adhesive force during pull-off was 471 ± 18.6 pN, smaller than the value observed for sample Ti-14C (low graft density). The disappearance of the JTC force and weaker adhesive force indicated that the brushes served as a barrier in preventing the interaction between the underlying hydrophobic surface and AFM tips. These results are consistent with our previously reported results on a different polymer brush system.[33]

Figures 7D and 7F show the representative AFM force curves and probability distribution histograms for the maximum adhesive force, respectively, for sample Ti-4C-P (high graft density). The AFM force curves for the samples coupled with peptides showed completely different profiles. Steric force was not observed when the AFM tip approached the surface. The attractive force ruptured at a shorter distance during pulling off. The brushes became more hydrophobic after incorporating peptides, consistent with the water contact angle measurements (Table 3). Similar force curves were obtained for the sample Ti-14C-P (Figure 7B). A relatively large adhesive force (972 ± 18.8 pN) was obtained when the tip was retracted from the low graft density brush conjugated with peptides compared to brush structure without peptides. The attractive force observed at a short distance might be due to the interaction between peptides and the AFM tips. The histogram of the maximum adhesive force was also similar to a higher adhesive force compared to the brush without peptides. The adhesive nature of low graft density brush is known to influence the nature of its interactions with proteins and cells as reported previously.[33] Such low graft density brushes will adhere more cells compared to a surface with high graft density brushes. We have seen the high density brushes produced better antimicrobial properties compared to low graft density brushes (Figure 5A). The high density brush (Ti4C-P) was less adhesive (889 ± 16.7 pN) compared to low density brush (Ti14C-P, 972 ± 18.8 pN) even though the peptide surface density (peptide is more hydrophobic) was higher in the prior case. The improved antimicrobial activity of the high density brushes was due to a combination of high peptide density on the surface as well as the nonadhesive nature of the peptide conjugated high density brush surface. Since bacterial debris do not accumulate on this surface due to the steric repulsion (as well as the nonadhesive nature) of high density brush, the surface-attached peptide would have better chance of interaction with bacteria. Since the bacterial killing action of surface-attached peptides is by the electrostatic disturbance of the bacterial membrane,[24,43,44] a coating with minimum adhesion and high peptide density might produce a better antimicrobial surface.

4. CONCLUSIONS

We have presented a method for one end grafting of the antimicrobial peptide Tet213 on amine-functionalized copolymer brushes on Ti surface. We found that the composition and the brush properties, such as graft density and thickness, influence the peptide grafting on to the surface. We have designed a method to calculate the peptide density and number of peptides grafted per polymer chain from the measured thickness of the grafted layer. The dry thickness of the copolymer brushes and peptide grafted brushes were confirmed using AFM analysis. The peptide density on the surface depended on the graft density as well as the composition of brushes. Using a cysteine-functionalized antimicrobial peptide Tet213, we

showed that graft density and peptide density are two important parameters in achieving the optimum antimicrobial properties of the peptide grafted polymer brush. These parameters can be easily modified by optimizing the surface-initiated copolymerization. Many fold higher peptide densities on the surface can be achieved when the brush layer was used for peptide conjugation compared to direct grafting of peptides on the surface. AFM analysis showed that the peptide grafted surface was more hydrophobic than brush alone and was consistent with the water contact angle measurements. Low graft density brushes are more adhesive than high graft density brushes even though the high graft density brush has more peptide surface density. A surface having low hydrophobic adhesion showed better antimicrobial properties. The peptide grafted brushes showed different surface features compared to brushes without peptides.

■ ASSOCIATED CONTENT

Supporting Information

Figures showing FTIR, XPS, fluorescence, and NMR analyses data of the samples; a detailed model for the calculation of peptide density. This material is available free of charge via the Internet at http://pubs.acs.org.

■ AUTHOR INFORMATION

Corresponding Author

*E-mail: jay@pathology.ubc.ca. Phone: 1-604-822-7085. Fax: 1-604-822-7742.

■ ACKNOWLEDGMENTS

This research was funded by the Canadian Institutes of Health Research (CIHR)−Natural Sciences and Engineering Research Council (NSERC) of Canada through collaborative health research projects (CHRP). The authors thank the LMB Hubs at the UBC Centre for Blood Research for the use of their research facilities; the infrastructure facility is supported by the Canada Foundation for Innovation (CFI) and the Michael Smith Foundation for Health Research (MSFHR). R.E.W.H. holds a Canada Research Chair. J.K. was a fellow of the Canadian Cystic Fibrosis Foundation. J.N.K. is a recipient of a CIHR/CBS New Investigator in Transfusion Science and MSFHR Career Investigator Award. K.Y. is a recipient of a CIHR/Canadian Blood Services (CBS) postdoctoral fellowship in Transfusion Science.

■ REFERENCES

(1) Darouiche, R. O. *N. Engl. J. Med.* **2004**, *350*, 1422−1429.
(2) Darouiche, R. O. *Clin. Infect. Dis.* **2001**, *33*, 1567−1572.
(3) Pulcini, E. L.; James, G. Biofilms and device implants. In *Applied Biomedical Microbiology*; Paulson, D. S., Ed.; CRC Press: Boca Raton, FL, 2009; Chapter 5.
(4) Costerton, J. W.; Stewart, P. S. *Science* **1999**, *284*, 1318−1322.
(5) Zimmerli, W.; Trampuz, A.; Ochsner, P. E. *N. Engl. J. Med.* **2004**, *351*, 1645−1654.
(6) Foxman, B. *Am. J. Med.* **2002**, *113*, 5−13.
(7) Matl, F. D.; Obermeier, A.; Repmann, S.; Friess, W.; Stemberger, A.; Kuehn, K. D. *Antimicrob. Agents Chemother.* **2008**, *52*, 1957−1963.
(8) Noimark, S.; Dunnill, C. W.; Wilson, M.; Parkin, I. P. *Chem. Soc. Rev.* **2009**, *38*, 3435−3548.
(9) Neil, A. *Polym. Chem.* **2010**, *1*, 769−777.
(10) Barbey, R.; Lavanant, L.; Paripovic, D.; Schuwer, N.; Sugnaux, C.; Tugulu, S.; Klok, H.-A. *Chem. Rev.* **2009**, *109*, 5437−5527.
(11) Hucknall, A.; Rangarajan, S.; Chilkoti, A. *Adv. Mater.* **2009**, *21*, 2441−2446.
(12) Gautrot, J. E.; Trappmann, B.; Oceguera-Yanez, F.; Connelly, J.; He, X.; Watt F. M. Huck, W. T. S. *Biomaterials* **2010**, *31*, 5030−5041.
(13) Emmenegger, C. R.; Brynda, E.; Riedel, T.; Sedlakova, Z.; Houska, M.; Alles, A. B. *Langmuir* **2009**, *25*, 6328−6333.
(14) Zhang, Z.; Zhang, M.; Chen, S. F.; Horbett, T. A.; Ratner, B. D.; Jiang, S. Y. *Biomaterials* **2008**, *29*, 4285−4291.
(15) Feng, W.; Brash, J. L.; Zhu, S. P. *Biomaterials* **2006**, *27*, 847−855.
(16) Trmcic-Cvitas, J.; Hasan, E.; Ramstedt, M.; Li, X.; Cooper, M. A.; Abell, C.; Huck, W. T.; Gautrot, J. E. *Biomacromolecules* **2009**, *10*, 2885−2594.
(17) Lai, B. F. L.; Creagh, L. A.; Janzen, J.; Haynes, C. A.; Brooks, D. E.; Kizhakkedathu, J. N. *Biomaterials* **2010**, *31*, 6710−6718.
(18) Raynor, J. E.; Petrie, T. A.; Garcia, A. J.; Collard, D. M. *Adv. Mater.* **2007**, *19*, 1724−1728.
(19) Navarro, M.; Benetti, E. M.; Zapotoczny, S.; Planell, J. A.; Vancso, G. J. *Langmuir* **2008**, *24*, 10996−11002.
(20) Onaizi, S. A.; Leong, S. S. J. *Biotechnol. Adv.* **2011**, *29*, 67−74.
(21) Hancock, R. E. W.; Sahl, H. G. *Nature Biotechnol.* **2006**, *24*, 1551−1557.
(22) Scott, M. G.; Dullaghan, E.; Mookherjee, N.; Glavas, N.; Waldbrook, M.; Thompson, A.; Wang, A.; Lee, K.; Doria, S.; Hamill, P.; Yu, J. J.; Li, Y. X.; Donini, O.; Guarna, M. M.; Finlay, B. B.; North, J. R.; Hancock, R. E. W. *Nature Biotechnol.* **2007**, *25*, 465−472.
(23) Hilpert, K.; Volkmer−Engert, R.; Walter, T.; Hancock, R. E. W. *Nature Biotechnol.* **2005**, *23*, 1008−1012.
(24) Hilpert, K.; Elliott, M.; Jenssen, H.; Kindrachuk, J.; Fjell, C. D.; Korner, J.; Winkler, D. F.; Weaver, L. L.; Henklein, P.; Ulrich, A. S.; Chiang, S. H.; Farmer, S. W.; Pante, N.; Volkmer, R.; Hancock, R. E. *Chem. Biol.* **2009**, *16*, 58−69.
(25) Gao, G.; Lange, D.; Hilpert, K.; Kindrachuk, J.; Zou, Y.; Cheng, J. T.; Kazemzadeh-Narbat, M.; Yu, K.; Wang, R.; Straus, S. K.; Brooks, D. E.; Chew, B. H.; Hancock, R. E.; Kizhakkedathu, J. N. *Biomaterials* **2011**, *32*, 3899−3909.
(26) Blin, T.; Purohit, V.; Leprince, J.; Jouenne, T.; Glinel, K. *Biomacromolecules* **2011**, *12*, 1259−1264.
(27) Glinel, K.; Jonas, A. M.; Jouenne, T.; Leprince, J.; Galas, L.; Huck, W. T. S. *Bioconjugate Chem.* **2009**, *20*, 71−77.
(28) Xiao, S. J.; Textor, M.; Spencer, N. D.; Weiland, M.; Keller, B.; Sigrist, H. *J. Mater. Sci.: Mater. Med.* **1997**, *8*, 867−872.
(29) Zou, Y.; Kizhakkedathu, J. N.; Brooks, D. E. *Macromolecules* **2009**, *42*, 3258−3268.
(30) Florin, E. L.; Rief, M.; Lehmann, H.; Ludwig, M.; Dornmair, C.; Moy, V. T.; Gaub, H. E. *Biosens. Bioelectron.* **1995**, *10*, 895−901.
(31) Wang, M.; Cao, Y.; Li, H. B. *Polymer* **2006**, *47*, 2548−2554.
(32) Ducker, W. A.; Sendan, T. J.; Pashley, R. M. *Langmuir* **1992**, *8*, 1831−1836.
(33) Zou, Y.; Rossi, N. A. A.; Kizhakkedathu, J. N.; Brooks, D. E. *Macromolecules* **2009**, *42*, 4817−4828.
(34) Wu, T.; Efimenko, K.; Vlcek, P.; Subr, V.; Genzer, J. *Macromolecules* **2003**, *36*, 2448−2451.
(35) Soto-Cantu, E.; Lokitz, B. S.; Hinestrosa, J. P.; Deodhar, C.; Messman, J. M.; Ankner, J. F.; Kilbey, S. M. II *Langmuir* **2011**, *27*, 5986−5996.
(36) Murata, H.; Prucker, O.; Ruehe, J. *Macromolecules* **2007**, *40*, 5497−5503.
(37) Kizhakkedathu, J. N.; Brooks, D. E. *Macromolecules* **2003**, *36*, 591−598.
(38) Iwata, R.; Satoh, R.; Iwasaki, Y.; Akiyoshi, K. *Colloids Surf., B* **2008**, *62*, 288−298.
(39) Husemann, M.; Malmstrom, E. E.; McNamara, M.; Mate, M.; Mecerreyes, D.; Benoit, D. G.; Hedrick, J. L.; Mansky, P.; Huang, E.; Russell, T. P.; Hawker, C. J. *Macromolecules* **1999**, *32*, 1424−1431.
(40) Zou, Y.; Lam, A.; Brooks, D. E.; Srikantha, P. A.; Kizhakkedathu, J. N. *Angew. Chem., Int. Ed.* **2011**, *50*, 5116−5119.
(41) Harris, B. P.; Kutty, J. K.; Fritz, E. W.; Webb, C. K.; Burg, K. J. L.; Metters, A. T. *Langmuir* **2006**, *22*, 4467−4471.

(42) Wieczorek, M.; Jenssen, H.; Kindrachuk, J.; Scott, W. R.; Elliott, M.; Hilpert, K.; Cheng, J. T.; Hancock, R. E.; Straus, S. K. *Chem. Biol.* **2010**, *17*, 970−980.
(43) Jelokhani-Niaraki, M.; Prenner, E. J.; Kay, C. M.; McElhaney, R. N.; Hodges, R. S. *J. Pept. Res.* **2002**, *60*, 23−36.
(44) Resende, J. M.; Moraes, C. M.; Munhoz, V. H.; Aisenbrey, C.; Verly, R. M.; Bertani, P.; Cesar, A.; Pilo-Veloso, D.; Bechinger, B. *Proc. Natl. Acad. Sci. U. S. A.* **2009**, *106*, 16639−16644.